

Morphological Transition of *Isotactic* Polybutene-1 Tetragonal Crystals: Optical and Transmission Electron Microscopy Observation

Motoi Yamashita* and Takuya Takahashi

Department of Bioscience and Bioinformatics, Ritsumeikan University, 1-1-1 Noji-higashi, Kusatsu, Shiga, 525-8577 Japan

The morphology and lateral growth rate of *isotactic* polybutene-1 (*it*-PB1) have been investigated for crystallization from the melt over a wide range of crystallization temperature from 50 to 111.9°C. The morphology of *it*-PB1 crystals is rounded shape at crystallization temperatures lower than 85°C, while lamellar single crystals possess faceted morphology at higher crystallization temperatures; the kinetic roughening transition occurs around 85°C. The nucleation and growth mechanism for crystallization does not work below 85°C, since the growth face is rough. However, the growth rate shows the supercooling dependence derived from the nucleation and growth mechanism; the nucleation theory seems still to work even for rough surface growth. Possible mechanisms for the crystal growth of polymers are discussed.

Keywords *isotactic* polybutene-1; tetragonal; growth rate, morphology, kinetic roughening; entropic barrier

1. Introduction

For polymers as well as low-molecular-weight materials, crystallization mechanisms have been investigated through the morphology and growth rate of crystals. An important feature specific to polymer crystallization is the supercooling dependence of the growth rate of the crystals. For faceted crystals, the growth rate G observed can be expressed as follows,

$$G = G_0 \exp\left[-\frac{U}{R(T - T_V)}\right] \exp\left[-\frac{K}{T\Delta T}\right] \quad (1)$$

where K is a constant, U is the 'activation' energy for polymer diffusion, $R = kN_A$, (k is the Boltzmann constant and N_A is Avogadro's number) T_V is the Vogel temperature ($= T_g - 30$ (K), T_g is the glass transition temperature), $\Delta T = T_m^0 - T$ is a supercooling (T_m^0 is the equilibrium melting temperature). G_0 is a factor almost independent of ΔT , the first exponential factor is the Vogel–Fulcher factor for viscosity, and the second exponential factor is the surface kinetic factor derived originally from the nucleation theory of Lauritzen–Hoffman assuming flat growth faces [1].

The thickness of the lamellar crystals is another important quantity describing the morphology specific to polymer crystals. It is well known that the thickness l decreases with supercooling ΔT [1],

$$l = \frac{2\sigma_e}{\Delta g} + \delta = \frac{2\sigma_e T_m^0}{\Delta h_f \Delta T} + \delta \quad (2)$$

where σ_e is the surface free energy of the lamellar surface, Δh_f is the heat of fusion per unit volume of crystal, Δg is the difference of free energies between crystal and liquid, namely, the driving force of crystallization, which is proportional to supercooling ΔT , and δ is a constant length independent of supercooling. The first term in Eq. (2) is the minimum thickness for the lamellar crystal to grow; the crystal with this thickness is in equilibrium with the melt in a supercooling of ΔT . Equation (2) has a clear meaning that the lamellar thickness of a growing crystal must be thicker by δ than the minimum thickness.

* Corresponding author: e-mail: motoi-y@is.ritsumei.ac.jp, Phone: +81 775661111 Ext.6489

We have investigated the crystallization of *it*-PB1 in the melt [2,3]. *It*-PB1 exhibits stable trigonal form (I) with 3/1 helical chains and metastable tetragonal form (II) with 11/3 helical chains as the most common structures. Crystallization in the bulk melt under atmospheric pressure yields the tetragonal form [4]. When stored at room temperature, the tetragonal phase undergoes a solid-solid transformation into the trigonal phase [5,6]. In this paper, we focus on the crystallization of the form II crystals, and report the growth rate and morphology of *it*-PB1 form II crystals grown in the melt. We observed that Eq. (1) holds not only for faceted crystals with flat growth faces but also for rounded crystals with kinetically roughened growth faces. We will discuss the possible mechanisms for the crystal growth taking account of the entropic barrier. The concept of the entropic barrier was originally proposed by Sadler [7] for polymer crystallization, partially adopted by Hoffman and Miller recently [8], and also described in a textbook of crystal growth by Chernov [9].

2. Experimental

The *it*-PB1 used in this study were purchased from Shell ($M_w \cong 185,000$; melt index is 20g/10min). *In-situ* observations of the crystallization process were carried out using an optical microscope (Nikon OPTIPHOT2) with a hot-stage (Mettler FP82). Films of *it*-PB1, *ca.* 50 μm thick, between two cover glasses were melted at 140°C for 2 min and cooled to a crystallization temperature between 52°C and 111.9°C. The growth rate was determined from the time dependence of the radius of spherulites or the major axis of axialites.

Wide angle X-Ray scattering (WAXS) was performed to identify crystal structures, using an imaging plate system (Rigaku R-AXIS DSII). Isotropic two-dimensional intensity collected was averaged to give the one-dimensional data, and corrected for the Lorentz factor. X-Ray used was nickel-filtered CuK_α radiation.

For the experiments of morphology observation, thin *it*-PB1 films were prepared by casting a *p*-xylene solution (0.1 wt% *it*-PB1) onto a carbon-coated mica. The films dried was heated up to 140°C, cooled to a crystallization temperature and crystallized in the hot-stage for a suitable time, and quenched to room temperature. The *it*-PB1-carbon films were floated on a water surface and picked up on electron microscope grids. The *it*-PB1 crystals on the carbon film were observed by transmission electron microscopy (TEM; JEOL Ltd. JEM-1200EX II) and optical microscopy (OM) to investigate the morphology of crystals.

3. Results

3.1 Growth rate

We confirmed by WAXS measurements that samples immediately after the crystallization are in form II. Hence, the observed growth rate and crystal morphology are those of crystals in form II. Typical optical micrographs of *it*-PB1 crystals grown from the melt are shown in Fig. 1. At crystallization temperatures higher than 90°C, tetragonal, octagonal, oval and circular crystals were usually observed; they are axialites, some of which grew to be circular crystals. At lower crystallization temperatures, spherulites were always observed. The size of the crystals $2R$, *i.e.*, the diameter of spherulites or the major axis of axialites, was measured as a function of time t .

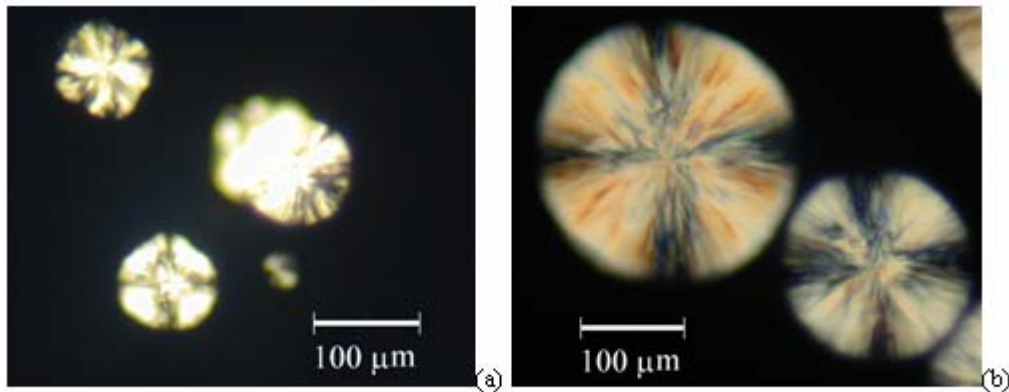


Fig. 1 Optical micrographs of *i*-PB1 crystallized in the melt at 90°C; crossed polars. (a) 3 min and (b) 8 min after the temperature reached 90°C.

The radius of the spherulites or the axialites R increased linearly with crystallization time t for all crystallization temperatures as shown in Fig. 2. The growth rate G was determined from the slope of the time-radius curve. The logarithm of G is plotted against crystallization temperature in Fig. 3. The results by Icenogle [10] are included for the sake of comparison. The $\log G$ - T curve is a half of the typical dome shape.

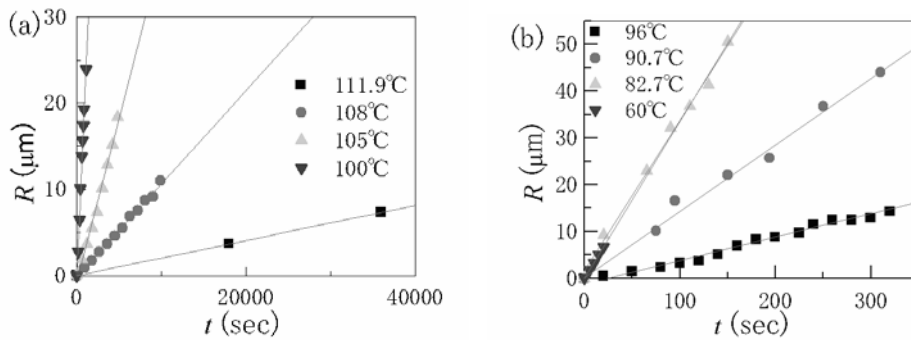


Fig. 2 Time dependence of radius R for several crystallization temperatures. (a): (■) 111.9°C, (●) 108°C, (▲) 105°C, (▼) 100°C. (b): (■) 96°C, (●) 90.7°C, (▲) 82.7°C, (▼) 60°C.

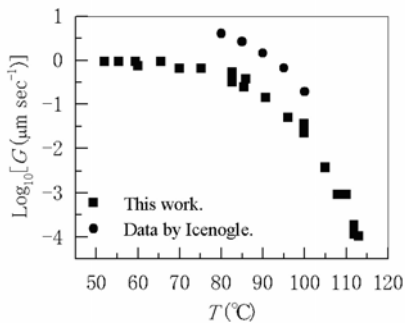


Fig. 3 Growth rate G versus crystallization temperature T : (■) this work and (●) data by Icenogle [10].

Figure 4 shows $\{\ln G + U/R(T - T_v)\}$ as a function of $1/\Delta T$. $\{\ln G + U/R(T - T_v)\}$ depends on $1/T\Delta T$ linearly over the whole range examined; Equation (1) holds for all the crystallization temperature range investigated from 52 to 111.9°C.

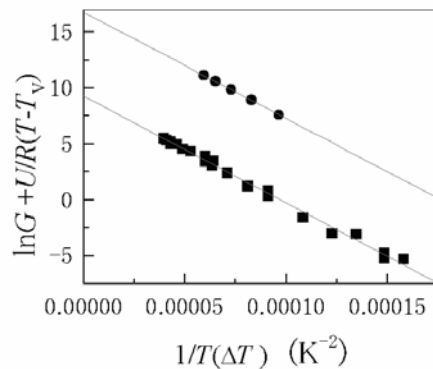


Fig. 4 Plot of $\ln G + U/R(T-T_v)$ versus $1/T\Delta T$. Symbols are the same as in Figure 3. The parameters used for the plots are as follows: $T_m^0 = 128^\circ\text{C}$, $T_v = -84.2^\circ\text{C}$, $U/R = 758$ [1].

According to Eq. (1), the extrapolation to zero of the straight line in Fig. 4 for $1/T\Delta T$ gives the value of $G_0 = 1.05 \times 10^4 \mu\text{m sec}^{-1}$; from the slope the value of K is obtained to be $9.54 \times 10^4 \text{K}^2$. The values of G_0 and K obtained from the data by Icenogle are $1.86 \times 10^4 \mu\text{m sec}^{-1}$ and $9.49 \times 10^4 \text{K}^2$, respectively. The value of K agrees well with the present result. The difference in the values of G_0 can be attributed to that of the molecular weight ($M_w = 750000$).

3.2 Morphology

Figure 5 shows the electron micrograph and diffraction pattern of a single crystal grown at 100°C ; optical micrograph of a single crystal grown at 100°C is also shown. The net pattern with four-fold symmetry in Fig. 5b shows the crystal in Fig. 5a is a flat-on tetragonal single crystal. The trace of well faceted $\{100\}$ growth front is observed clearly in Fig. 5a; the traces of facets appear even more clearly in the optical micrograph (Fig. 5c). Also observed are the sector boundaries of $\{110\}$. The traces of growth fronts in Figs. 5a and 5c indicate that the tetragonal single crystals are well faceted at 100°C , and hence the tetragonal crystals grow by nucleation-controlled growth on $\{100\}$ plane at 100°C . Similar faceted morphology is observed in crystals grown at 110°C and 88°C in the melt (figures not shown).

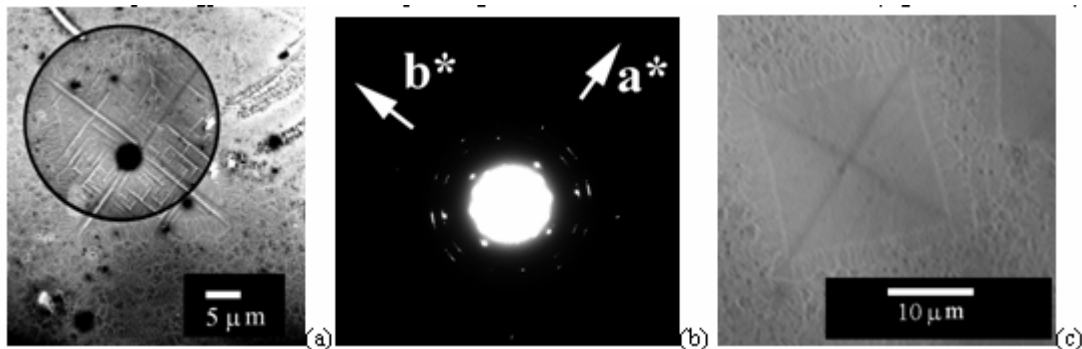


Fig. 5 (a) Electron micrograph and (b) diffraction pattern of *it*-PB1 single crystal grown at 100°C . The solid circle in (a) shows the selected area for the diffraction. (c) Optical micrograph of an *it*-PB1 single crystal grown at 100°C .

On the contrary, at a lower temperature of 85°C , the growth front shows a rounded and wavy habit, indicating the growth face is kinetically roughened (Fig. 6).

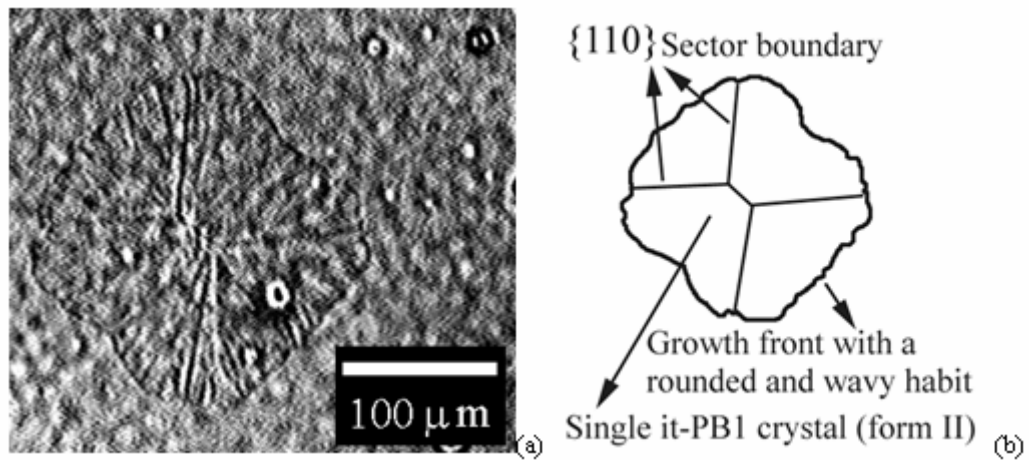


Fig. 6 (a) *In-situ* optical micrograph and (b) schematic illustration of an *it*-PB1 single crystal growing at 85°C.

Therefore, *it*-PB1 tetragonal crystals have the kinetic roughening transition temperature around 85°C; the growth mechanism changes from nucleation controlled to adhesive growth at crystallization temperatures lower than 85°C since the growth face becomes rough on the molecular scale. This is, however, in contradiction with the single linear dependence of $\{\ln G + U/R(T - T_v)\}$ on $1/\Delta T$ observed in Fig. 4: the $1/\Delta T$ dependence of $\{\ln G + U/R(T - T_v)\}$ does not show any transition. The same disagreement between the growth rate and morphological change is reported by Tanzawa *et al.* in the crystal growth of *isotactic* polystyrene in solution and in the melt [11, 12].

4. Discussion

According to the traditional theory of crystal growth, the growth of a faceted crystal is controlled by secondary nucleation. Hence, it is reasonable that Eq. (1), derived from the nucleation theory, holds for the growth of faceted crystals of *it*-PB1 grown at low supercoolings. However, in the experiments above, it is shown that Eq. (1) holds for all crystallization temperatures, including the kinetic roughening temperature. Therefore, Eq. (1), derived from the nucleation theory, holds for nucleation-controlled growth and rough-surface growth; Equation (1) is universal for polymer crystallization. Also, Eq. (2) is universal; ΔT determines the thickness l of all the lamellar crystals independent of the morphology. For the rough-surface growth from the melt, we have the Wilson–Frenkel formula [13],

$$G = G_0 \exp\left[-\frac{U}{R(T - T_v)}\right] \left\{1 - \exp\left[-\frac{\Delta g}{kT}\right]\right\} \quad (3)$$

where the viscosity factor is modified for polymers. This equation shows that for high supercoolings ($\Delta g \gg kT$), the growth rate G is almost independent of supercooling ΔT , and hence, Eq. (3) cannot apply to the rough surface growth in polymer crystallization. However, as described in the textbook of Chernov,[9] if the activated state of a crystallizing segment just before attachment to the growth face implies the loss of entropy in the melt, G_0 includes a factor $\exp(-\Delta S_m/k)$; where ΔS_m is the entropy of melting. We here assume that ΔS_m is proportional to the lamellar thickness l ; this is a generalization of the entropic barrier for the first stem deposition on the growth face, described in the recent version [8] of the L–H theory, to that for the deposition of stems later than the first stem (Fig. 7). Since l is inversely proportional to ΔT , with this activation state we can roughly reproduce the ΔT dependence of growth rate observed in the experiment: a straight line in the plot of $\{\ln G + U/R(T - T_v)\}$ versus $1/T\Delta T$ for the crystallization of faceted and rough-surface crystals. The important parameter K in Eq. (1) is, however, different from that in the L–H theory.

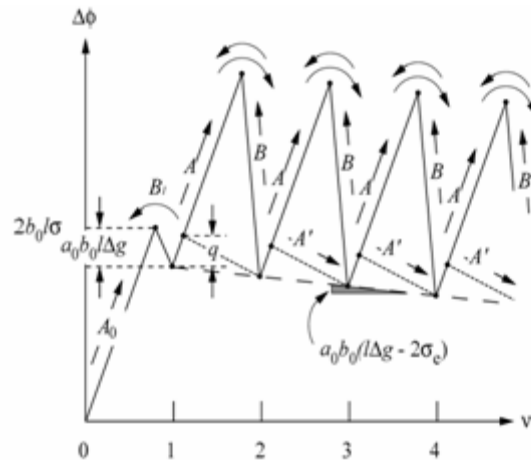


Fig. 7 Free energy barrier system for the deposition of chain stems with a length l into a flat growth face. The original figure in reference [8] (the dotted lines) is modified for $\nu > 1$: $\Delta\phi$ is the free energy of formation of a new layer comprised of ν stems, A_0 and A' are forward rate constants of L-H theory. A is that in the present model, B and B_1 are backward rate constants. $\Delta\phi$ is described with stem length l , width of stem a_0 , layer thickness b_0 , lateral surface free energy σ , fold surface free energy σ_e , work of chain folding q , and the difference of free energies between crystal and liquid Δg .

5. Conclusion

1. Kinetic roughening transition was observed around 85°C in the crystallization of *it*-PB1 form II crystals from the melt; a flat growth face, facet, required for nucleation theory does not exist below 85°C. On the other hand, the temperature dependence of growth rate followed the nucleation theory in the temperature range of 52 to 111.9°C. Equation (1) holds for the faceted and rough-surface crystals.
2. The traditional theory for rough-surface growth gives Eq. (3); in the equation, the “preexponential factor” G_0 includes $\exp(-\Delta S_m/k)$ where the entropy of melting ΔS_m is assumed to be proportional to the lamellar thickness l .
3. Equation (3) with G_0 modified in accordance with the above can plausibly describe the ΔT dependence of growth rate given by Eq. (1).

Acknowledgements The author M.Y. expresses his sincere thanks to Professor Fukao of Ritsumeikan University for valuable pieces of advice and encouragement.

References

- [1] J. D. Hoffman, G.T. Davis and J.I. Lauritzen Jr., The rate of crystallization of linear polymers with chain folding. *Treatise on Solid State Chemistry*; Plenum Press: New York, 497–614 (1976).
- [2] M. Yamashita and M. Kato, *J. Appl. Cryst.* **40**, s650 (2007).
- [3] M. Yamashita, A. Hoshino and M. Kato, *J. Polym. Sci. Polym. Phys. Ed.*, in printing (2007).
- [4] A. Turner-Jones, *J Polym Sci Part B: Polym Lett*, **1**, 455 (1963).
- [5] G. Natta, P. Corradini and I. W. Bassi, *Nuovo Cimento Suppl*, **15**, 52 (1960).
- [6] G. Natta and P. Corradini, *Nuovo Cimento Suppl*, **15**, 465 (1960).
- [7] D.M. Sadler, *Polymer* **24**, 1401 (1983).
- [8] J. D. Hoffman and R.L. Miller, *Polymer* **38**, 315 (1997).
- [9] A.A. Chernov, *Growth Mechanisms in Modern Crystallography III*; Springer: New York, 104–158 (1984).
- [10] R. D. Icenogle, *J. Polym. Sci. Polym. Phys. Ed.*, **23**, 1369 (1985).
- [11] Y. Miyamoto, Y. Tanzawa, H. Miyaji and H. Kiho, *J. Phys. Soc. Jpn*, **58**, 1879 (1989).
- [12] Y. Tanzawa, *Polymer*, **33**, 2659 (1992).
- [13] Y. Saito, *Statistical Physics of Crystal Growth*; World Scientific Publishing Co. Pte. Ltd. (1996).